Colloids and Surfaces A: Physicochem. Eng. Aspects 473 (2015) 32–39

Contents lists available at ScienceDirect

Colloids and Surfaces A: Physicochemical and Engineering Aspects

journal homepage: www.elsevier.com/locate/colsurfa

In situ measurement of the permeability of foam films using quasi-two-dimensional foams

L. Saulnier[a,1], W. Drenckhan[a], P.-E. Larré[a,2], C. Anglade[a,3], D. Langevin[a], E. Janiaud[b], E. Rio[a,*]

[a] Laboratoire de Physique des Solides, Université Paris-Sud, UMR CNRS 8502, Bâtiment 510, 91405 Orsay Cedex, France
[b] Saint-Gobain Recherche, Saint-Gobain Recherche, 39 quai Lucien Lefranc, 93303 Aubervilliers Cedex, France

HIGHLIGHTS

- We present a new method to measure the permeability of foam films in situ in a two-dimensional foam.
- We examine the influence of the liquid fraction and show that it can be taken into account through geometrical considerations only.
- We examine the influence of the gas and show that we recover results obtained in the literature at the scale of an isolated film.

GRAPHICAL ABSTRACT

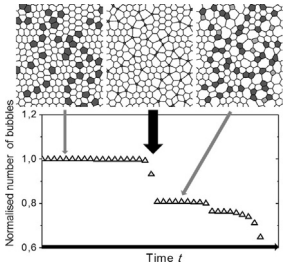

ARTICLE INFO

Article history:
Received 15 October 2014
Received in revised form 7 January 2015
Accepted 8 January 2015
Available online 17 January 2015

Keywords:
2D foams
Coarsening
Foam film permeability

ABSTRACT

The gas permeability of the thin liquid films which separate neighbouring bubbles in a liquid foam plays a key role in foam coarsening. Different approaches have been developed in the past to measure the film permeability, relying on measurements either on individual films/bubbles or on bulk foams. While the first approach may not be sufficiently representative of a real foam film, the latter is hardly feasible due to a lack of quantitative description of the coarsening of bulk foams with non-negligible liquid content. Here we show that a good compromise between these approaches can be achieved by investigating the coarsening of quasi-two-dimensional foams. More precisely, we propose a particularly simple approach in which we follow the evolution of the number of bubbles of an initially monodisperse foam. In this case, a large number of bubbles disappear simultaneously, leading to a "catastrophic" event, which can be identified easily and accurately related to the film permeability. We demonstrate the potential of this technique by using aqueous foams stabilised by sodium dodecyl sulfate having different liquid fractions and containing different gases. The experiments are compared to Surface Evolver simulations.

© 2015 Elsevier B.V. All rights reserved.

* Corresponding author. Tel.: +33 1 69 15 69 60; fax: +33 1 69 15 60 86.
E-mail addresses: LSAULNIER@rd.loreal.com (L. Saulnier), wiebke.drenckhan@u-psud.fr (W. Drenckhan), Pierre.Larre@unitn.it (P.-E. Larré), anglade@insa-toulouse.fr (C. Anglade), dominique.langevin@u-psud.fr (D. Langevin), eric.janiaud@saint-gobain.com (E. Janiaud), rio@lps.u-psud.fr (E. Rio).
[1] Present address: L'Oréal Research & Innovation, 11-13 rue Dora Maar, 93400 Saint-Ouen, France.
[2] Present address: INO-CNR BEC Center and Dipartimento di Fisica, Università di Trento, Via Sommarive 14, I-38123 Povo, Italy.
[3] Present address: Laboratoire Matériaux et durabilité des constructions, INSA Toulouse, 135, Avenue de Rangueil, 31077 Toulouse Cedex 4, France.

http://dx.doi.org/10.1016/j.colsurfa.2015.01.009
0927-7757/© 2015 Elsevier B.V. All rights reserved.

1. Introduction

Liquid foams consist of closely packed gas bubbles which are surrounded by a continuous liquid phase and stabilised by surface active agents [1,2]. They are inherently unstable, leading to a continuous growth of the average bubble volume with time either via the rupture of the thin films separating two bubbles ("coalescence") or via the diffusion of gas through the thin films driven by pressure differences between neighbouring bubbles ("coarsening").

In order to understand the coarsening behaviour of a liquid foam, one needs to couple the gas transport through a single film with the distribution of film sizes and bubble pressures in the foam. Many different experiments have been developed in the past aiming to measure the permeability of an isolated film ([3] and references therein). These include in particular the "bubble diminishing method" [4–7] and a variant in which a pressure gradient across the film can be imposed explicitly [8–11]. We can also cite experiments performed in 1D-foams (bamboo foams: collection of bubbles in a tube) [12]. Even though these approaches have been quite successful in linking the permeability of the film to parameters like the film thickness or the physico-chemical parameters (nature and concentration of stabilising agents, nature of gas, additives, etc.), they remain somewhat simplistic and non-realistic models of real foam films. The collective effects as well as the topology of the foam are crucial to understand coarsening. For example, in isolated bubbles, the pressure across the liquid film which drives the coarsening is directly linked to the radius R of the bubble by the Laplace law ($\Delta P = 4\gamma/R$, with γ being the surface tension of the liquid), while in a foam with polyhedral bubbles the same Laplace law links the pressure drop directly to the topology of a bubble (here, the number of neighbours).

In order to access the permeability of the films in real foams, light scattering or tomographic techniques have been successfully used [13] to measure the characteristic time for coarsening. However, no particular attention was paid to the determination of foam film permeability. It was generally considered to be a parameter which depends mainly on foam film thickness. In more recent results, a dependence on the monolayer permeability was reported, as in model films [14]. However, in the experiments of reference [14], only the bubbles at the surface of the container were monitored, which could prevent to extract the averaged permeability in the whole foam.

Here we propose the systematic use of quasi-two-dimensional (quasi-2D) foams as a good compromise between single film/bubble and real foam experiments. Such quasi-2D foams are obtained by squeezing a monolayer of bubbles between two transparent plates. They have been used successfully in the past to reveal important foam properties, their key advantage being their straightforward visualisation and accurate theoretical description [2,15]. In particular, Roth et al. [16] have recently reported detailed investigations into the coarsening behaviour of such quasi-2D foams with different liquid fractions. Duplat et al did an extensive study of the evolution of a 2D monodisperse foam towards the scaling state through coarsening [28].

Here we propose that these foams may be used in an even more straightforward manner by simply measuring the time evolution of the number N of initially equal-volume bubbles contained in the cell. Even highly disordered quasi-2D foams consist of bubbles which mainly have either five, six or seven sides [17]. Following von Neuman's Law (Section 3), the gas exchange between the bubbles leads to a shrinkage of the 5-sided bubbles and a growth of the 7-sided bubbles, while the volume of the 6-sided bubbles remain unchanged. If topological rearrangements during the initial coarsening stage are negligible, then all the initially 5-sided bubbles disappear at the same moment. At this point the number of bubbles drop dramatically, which can be easily measured using simple image analysis software like ImageJ. This phenomenon is shown in Fig. 1 using Surface Evolver simulations [18] and experiments.

In the following we describe this approach in detail. After a description of the experimental set-up in Section 2 we continue with a short introduction to the theory of 2D foam coarsening (Section 3). We then discuss experimental results obtained for aqueous foams containing different amounts of liquid and surfactants (Section 5.2), and different gases (Section 5.3).

We find good agreement between our results and those obtained by the diminishing bubble method for the permeability of the films. The simplicity of our approach makes it attractive to easily and accurately measure the permeability of foam films over a wide range of parameters.

2. Materials and methods

2.1. Experimental setup and procedure

To study 2D foams, we use a cell made of two glass plates separated by a uniform thickness of 1 mm. Before use, the cell is immersed in Deconex 22LIQ-x diluted 30 times during 10 h. Then, it is rinsed 10 times with tap water, 10 times with distilled water and 5 times with double-distilled water (Millipore system, $\sigma = 18.2\ \mathrm{m\Omega\,cm}$). It is then soaked in double distilled water during 10 h. The tubes are rinsed in the same way. We use new syringes for each experiment. The cell is watertight thanks to two rubber joints separated by a silicon joint which ensures the tightness but never enters in contact with the foam. This is important since silicone is hydrophobic and leads to bubble bursting upon contact.

The cell is first set vertically and filled with the foaming solution. We measure the injected liquid volume V_{inj}, which corresponds to the volume of the cell. A known quantity of liquid V_{liq} is then removed through a syringe placed at the bottom of the cell which puts the cell at a pressure below ambient pressure. A second syringe is connected to a balloon containing the gas of interest (air, argon or nitrogen). The balloon is partially deflated to ensure that it is at ambient pressure. The gas replaces the removed liquid creating monodisperse bubbles of radius between 0.5 and 1 mm depending on the experiment. This procedure allows controlling the type of gas, the bubble size which is fixed by the size of the syringe and the liquid content of the foam which is defined by the liquid fraction

$$\Phi = \frac{V_{\mathrm{inj}} - V_{\mathrm{liq}}}{V_{\mathrm{inj}}}. \quad (1)$$

In our experiments the liquid fraction varies between 2% and 10%.

Once the desired liquid fraction is achieved, the syringes are sealed and the cell is set horizontally. The horizontality is ensured by a three feet support adjusted using a bubble level. The cell is lit by a circular neon allowing a homogeneous lighting of the foam (Fig. 2). A video of the foam ageing is recorded using a digital camera (uEye, lens with a focal of 12 mm), which allows taking high resolution pictures of the foam (3840*2748 pixels) at 1 frame/min.

To analyse the pictures of 2D foams, we use homemade plugins implemented in the free software ImageJ. These plugins allow us extracting the number of sides, the area and the perimeter of each bubble from a given picture. Three main steps are accomplished during the image analysis. The picture is first thresholded using grey level intensity in order to separate the wet walls (dark pixels) from the gas bubbles (bright pixels). Each bubble, constituted of connected pixel, is tagged with a single identifier. Secondly, the pixels from the walls are scanned and attached to a bubble only if they touch a single bubble. This operation leads step by step to a skeletonised 2D foam. At the end of this operation, vertices are

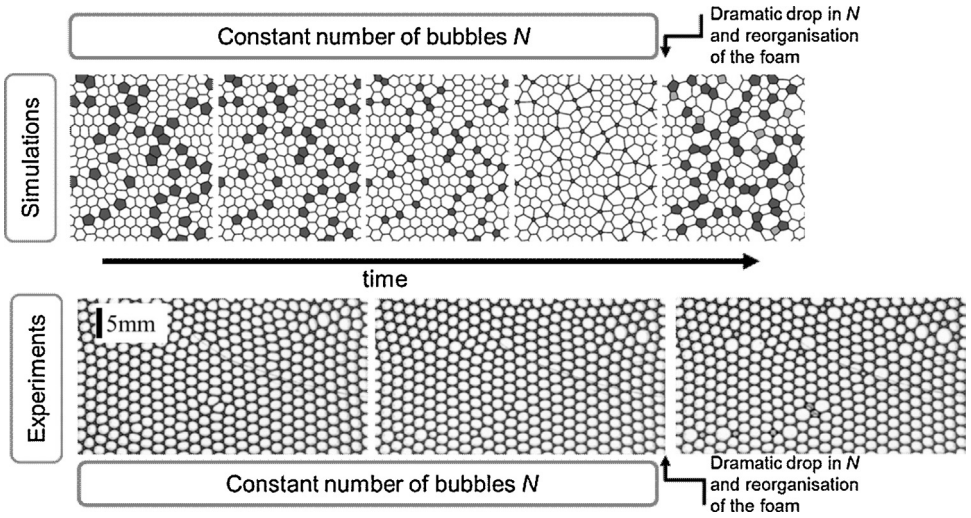

Fig. 1. Evolution of a disordered monodisperse 2D foam during coarsening: simulated with Surface Evolver (top row), observed experimentally (bottom). In both cases, all 5-sided bubbles (dark grey in the simulation) disappear simulataneously. This leads to a dramatic decrease in the number of bubbles which can be detected easily with automated image analysis.

the remaining wall pixels that are touching three different bubbles. Thirdly, the three neighbouring bubble index associated to each vertex is used to reconstruct the whole foam structure which enable us to process to the measurements.

2.2. Systems

We used two different foaming solutions. We first use a commercial solution (Fairy-Procter & Gamble) which is known to make very stable foams while it has a complex composition. The absence of bubble coalescence in foams generated from these solutions allows us testing the relevance of the proposed experiment. We then performed experiments with pure surfactant solutions, using different concentrations of sodium dodecyl sulfate (SDS). SDS is purchased from Sigma–Aldrich and used as received. Fresh solutions are prepared for each experiment to avoid the hydrolysis of the surfactant. The glassware is cleaned before use with the same protocol used with the glass cell (see Section 2.1). The SDS concentration is varied between 8.2 and 123 mM, which corresponds respectively to the critical micellar concentration (cmc) and to 15 cmc. In the following, all surfactant concentrations are given in multiples of the cmc.

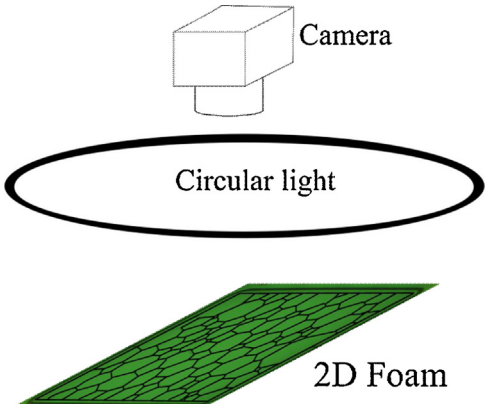

Fig. 2. Experimental setup: visualisation of the ageing of a 2D foam enlightened by a circular light spot.

2.3. Avoiding coalescence

One major concern of our experiment is to study coarsening only in the absence of any coalescence event. We therefore performed a preliminary study to identify a domain of liquid fraction and surfactant concentration in which foams experience only coarsening. To do so, we generated 2D foams having bubble size roughly constant ($R = 1.2 \pm 0.25$ mm), different liquid fractions (2–10%) and different SDS concentrations (1–15 cmc). We followed their ageing during 600 s. From visual observation, we were able to build a stability diagram represented in Fig. 3. We marked foams experiencing coarsening only (no coalescence event observed within 600 s) with empty diamonds and foams experiencing both coarsening and coalescence with filled diamonds. In Section 5, we will only present experiments performed with foams in which coalescence events were absent.

The diagram of Fig. 3 is a subject of interest in itself but beyond the scope of this paper. Nevertheless, let us make a quick comment of the results. We observe that coalescence appears only when the liquid fraction Φ is below a critical value. This is in line with previous studies suggesting that a critical liquid fraction sets

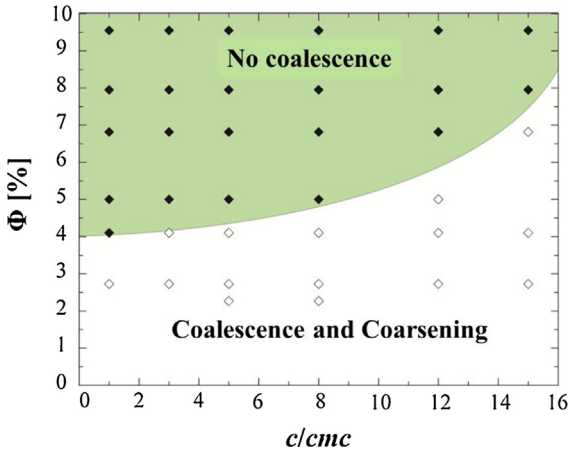

Fig. 3. Stability diagram for the competition between coarsening and coalescence in 2D SDS foams. The "no coalescence area" is defined such as no bubble coalescence is observed during the first 600 s of foam ageing. The bubble radius is between 1 and 1.5 mm.

the coalescence [19,20] but we measure much higher values of this critical liquid fraction, maybe because we are working on 2D foams. Nevertheless, the mechanism behind this observation is still unknown [21].

3. Theory

The main advantage of working with 2D foams is how well they are already described in the literature [2,15,28]. In particular, the coarsening of perfectly dry quasi-2D foams has been accurately accounted for by von Neumann [22]. The von Neumann's law describes the evolution of the area A_i of a bubble i in an infinite 2D foam due to the gas flux coming from its n_i neighbouring bubbles. Assuming that the gas diffuses only through the flat film of height e_F (Fig. 7), the temporal rate of change of A_i can be written as

$$\frac{\partial(eA_i)}{\partial t} = \frac{\partial V}{\partial t} = -\frac{\kappa}{P_i}\sum_{j=1}^{n_j} l_{ij} e_F (P_i - P_j), \tag{2}$$

where κ is the permeability of the film of length l_{ij} which separates the bubble i from one of his neighbour j ($j = 1, \ldots, n_i$), e is the plate spacing, e_F the film height and P_i (P_j) is the pressure in the bubble i (j). Note that κ is supposed to be the same for all the film and, thus to be independent of the film thickness, at least in the range of thicknesses present in the foam. The Laplace law quotes: $\Delta P = 2\gamma C = 2\gamma(1/R_1 + 1/R_2)$ with R_1 and R_2 the principal radius of curvature of the surface and γ the surface tension. Since it is a 2D foam, $1/R_2$ is equal to 0. Eq. (2) then becomes

$$\frac{\partial A_i}{\partial t} = -\frac{e_F}{e}\frac{2\gamma\kappa}{P_i}\sum_{j=1}^{n_j} l_{ij} C_{ij}, \tag{3}$$

where C_{ij} denotes the curvature of the film separating bubbles i and j. In a purely two-dimensional foam, the angle separating two adjacent films equals $2\pi/3$ (Plateau's law). It follows that:

$$2\pi = \frac{\pi}{3} n_i + \sum_{j=1}^{n_j} l_{ij} C_{ij}, \tag{4}$$

from which the von Neumann's law can easily be deduced

$$\frac{\partial A_i}{\partial t} = -\frac{e_F}{e}\frac{2\pi\gamma\kappa}{3P_i}(6 - n_i) = -D_{\text{eff}}(6 - n_i), \tag{5}$$

where D_{eff} is a diffusion coefficient taking into account not only the film permeability but also the pressure of the bubble, the surface tension and the separation between the two plates. The variation of the bubble volume then simply depends on the number of sides of the bubble. Bubbles with more than six sides will grow, bubbles with less than six sides will shrink and the size of those with six sides will remain unchanged. In the dry limit, the height of the film is simply the plate spacing so $e = e_F$.

4. Simulations

We used Surface Evolver [18] in the 2D-arc mode combined with a coarsening algorithm in order to investigate certain questions which were more difficult to explore by experiments. This concerned in particular the effect of disorder and polydispersity of the initially monodisperse foam on the presence of the catastrophic event.

For this purpose, we generated a check-board-like geometric grid with 900 fields (bubbles) using a home-made MATLAB code in order to obtain the bubble topology and the bubble-area constraints, which was then fed into the Surface Evolver. Surface Evolver was then used to relax the check-board bubble geometry

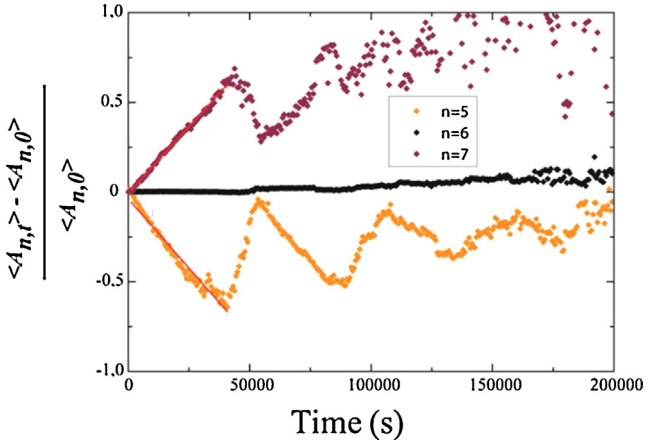

Fig. 4. Evolution of the normalised bubble area for bubbles with respectively five, six and seven sides. The experiments are performed with the commercial dishwashing liquid "Fairy" (Section 2.2). Bubbles radius $R = 1.5$ mm, $F = 5\%$.

while maintaining the constraints on the bubble area distribution. Different cut-off lengths were used during the relaxation, leading to foams with different degrees of disorder (as shown in Fig. 5(c)). The polydisperse foams where obtained by imposing area-constraints with a Gaussian distribution and a standard deviation of 30% in the case of Fig. 5(c).

Since Surface Evolver has access to the bubble pressures after the relaxation, coarsening is simulated using the same kind of diffusion equation as given in Eq. (2) applied to each element of the discretised films which separate bubbles. A more detailed account of the use of Surface Evolver for foam coarsening can be found in [23,24], we therefore only describe briefly the main concept: at each iteration and at each film element, we transfer a small amount of gas (area ΔA) which is proportional to the pressure drop ΔP across the film and a diffusion coefficient κ_{eff}, i.e. $\Delta A = -\kappa_{\text{eff}}\ \Delta P$ which is chosen sufficiently small so that the area change of each bubble during one iteration remains small in comparison to its total area. Once the area transfer has been performed at each film element, the foam is relaxed to its new equilibrium configuration. Bubbles which are smaller than 1/1000 of the initial bubble area are removed from the simulation. All quantities are dimensionless (average bubble area = 1, film tension = 1, etc.) and can be related to the physical experiments by proper dimensionalisation – which we verified. However, we did not follow up quantitative comparison between experiments and simulation since we were mostly interested by complementary exploration and illustration. A typical image sequence obtained by these simulations is shown at the top of Fig. 1.

5. Results

5.1. Proof of principle

Von Neumann's law (Eq. (5)) can be easily demonstrated in experiments. This is shown in Fig. 4 using a typical result of our experiments. The average of the visible area $\langle A_{n,t}\rangle$ of n-sided bubbles is normalised by the initial averaged size of the n-sided bubbles $\langle A_{0,t}\rangle$ and plotted versus time. One can see that at the beginning, the 5-sided bubbles shrink, the 7-sided bubbles grow and the size of the 6-sided bubbles does not change.

If we now focus on the 5-sided bubbles, it appears that after a time close to 50,000 s, almost all these bubbles disappear. Indeed, we work with monodisperse bubbles and they all shrink at the same rate so there is a "catastrophic time" at which they all disappear together. The only hypothesis is no rearrangements occur

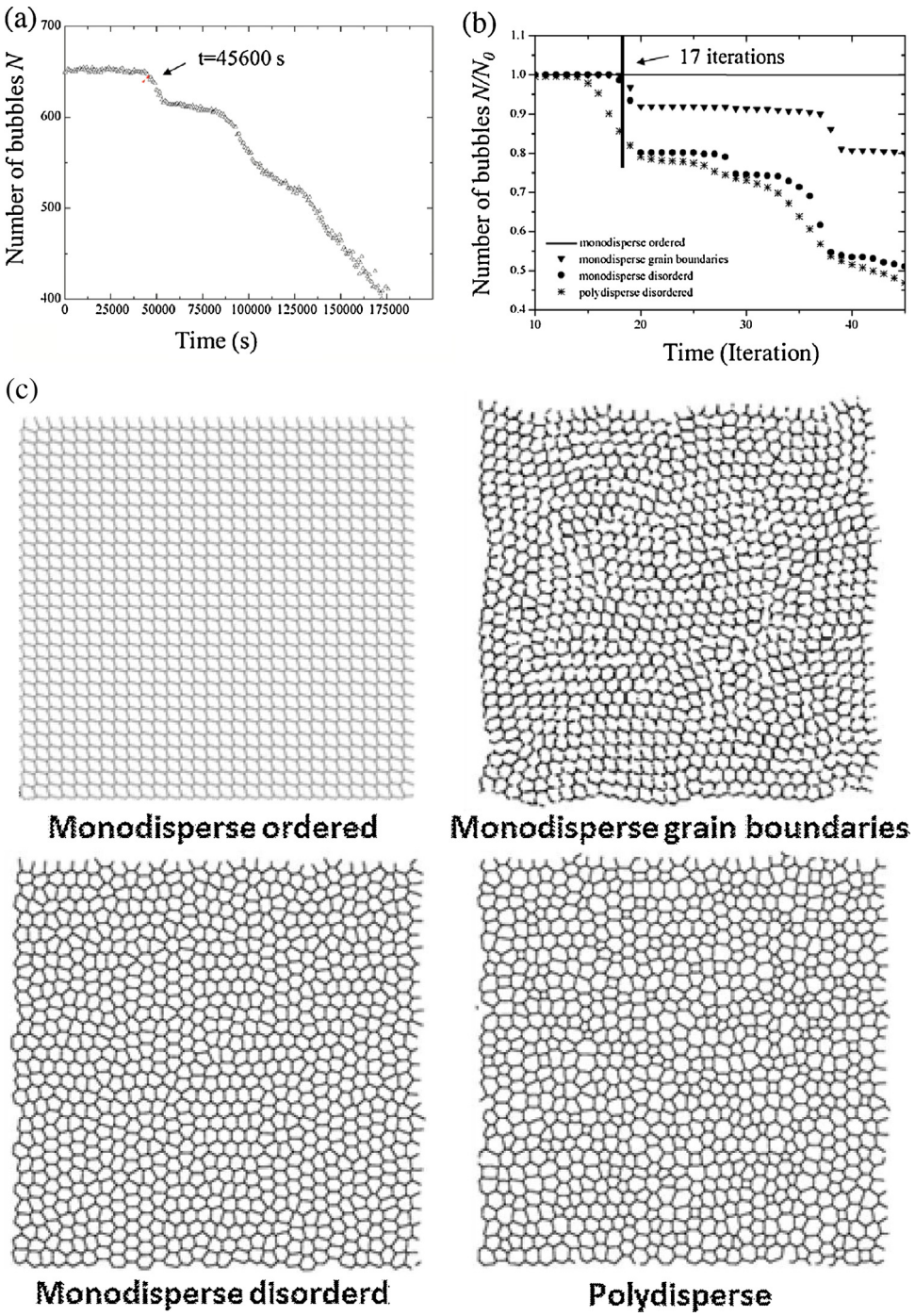

Fig. 5. Observation of the catastrophic event on both (a) experiments and (b) simulations containing $N_0 = 900$ bubbles. The experiments are performed with a commercial dishwashing liquid "Fairy", at a liquid fraction of 5% with an average bubble radius of 1.5 mm. (c) Different types of initial foams whose coarsening was studied using surface evolver simulations, leading to the data shown in (b).

during this first stage which would reshuffle the foam and hence the foam topology. The linear evolution of the normalised area with time, accordingly to Eq. (5) is a proof that this assumption is fulfilled, i.e. that the topological rearrangements are negligible. This is confirmed experimentally by direct visualisation. Right after the disappearance of all the 5-sided bubbles, a lot of re-arrangements occur leading to new 5-sided bubbles. A similar scenario applies to the 7-sided bubbles. After the catastrophic time, the coarsening follows Eq. (5) again until a second and sometimes a third catastrophic time. Nevertheless, the evolution of $(\langle A_{n,t} \rangle - \langle A_{n,0} \rangle)/\langle A_{n,0} \rangle$ with time is less and less linear, while approaching the scaling state. This is because the polydispersity increases so that more and moretopological events occur leading to a smoother and smoother behaviour, which will finally lead to the scaling state. In the following, we will thus focus one the first catastrophic time for a quantitative study of the coarsening.

This catastrophic time is then quite easy to observe visually since a lot of events occur after a quiet period of time. In particular, it can be determined easily by counting the number of bubbles versus time. As can be seen in Fig. 5(a), a large number of bubbles disappear at a given time. This means that the use of this method does not require an extensive treatment of the pictures but only a careful counting of the bubbles versus time. This last measurement is quite easy to perform. For example, there is a plugin which

is implemented in the native version of the free Software ImageJ which enables counting the evolution of the number of bubbles in a series of pictures. This result is confirmed by simulations (Fig. 5(b)), for which we use Surface Evolver [18], as briefly described in Section 4.

The simulations allow exploring the influence of different parameters on this catastrophic time. Of particular interest to us was the effect of initial disorder and polydispersity. The different initial foam structures whose coarsening behaviour we explored are shown in Fig. 5(c). These range from a perfectly ordered monodisperse foam, which does not coarsen at all, since all bubbles have six neighbours, to a disordered polydisperse foam. The cases in-between are monodisperse foams which either consist of ordered zones separated by grain boundaries, or are perfectly disordered. The increasing disorder and polydispersity of these foams leads to an increasing width of the distribution of the number of neighbours. While a monodisperse, ordered foam has only 6-sided bubbles, a monodisperse, disordered foam contains bubbles with five, six and seven neighbours. A polydisperse disordered foam contains also bubbles with less than five and more than seven neighbours, their numbers depending on the polydispersity. One can see in Fig. 5(b) that these changes in the neighbour distributions have an influence on how well the transition in the number of bubbles at the catastrophic event is defined without changing its absolute position. The transition is sharper with monodisperse foams and it is easier to define the catastrophic time in the presence of disorder, simply because there are more 5-sided bubbles in this case so the number of disappearing bubbles is more important. Foams obtained in the experiment are typically foams with ordered zones separated by grain boundaries.

The catastrophic time is directly linked to the diffusion coefficient D_{eff} defined in Eq. (5). This equation can be integrated and averaged over the different bubbles leading to

$$\langle A_{5,t}\rangle - \langle A_{0,t}\rangle = -D_{\text{eff}}(6 - n_i)t. \tag{6}$$

So, at the catastrophic time τ, $\langle A_{5,t}\rangle$ =0 and

$$D_{\text{eff}} = \frac{\langle A_{0,t}\rangle}{\tau}. \tag{7}$$

In the following, we will use this equation to measure the permeability of the foam films under different conditions. A second and sometimes a third drop of the number of bubbles can be observed (see Fig. 5) but the procedure using the first drop is more accurate. Note that Eq. (6) suggests that the slope of the linear part in Fig. 4 is also directly linked to the permeability. On the particular foam analysed in Fig. 4, both method respectively lead to $D_{\text{eff}} = 1.5\,\text{m}^2/\text{s}$ and $D_{\text{eff}} = 1.8\,\text{m}^2/\text{s}$. Thus, they agree qualitatively. In the following, we choose to use the method of the "catastrophic time" because it is easier to implement: it is only necessary to know the number of bubbles and not their respective number of neighbours.

5.2. Influence of the liquid fraction and of the surfactant concentration

We measured the effective diffusion coefficient D_{eff} for different liquid fractions Φ and for different concentrations of SDS above the cmc assuming at the outset that we are in the dry limit i.e. $e = e_F$ in Eq. (5). The obtained results can be seen in Fig. 6. The bubble size is $R = 0.6 \pm 0.07$ mm. We can observe (i) that the diffusion coefficient does not depend very strongly on the surfactant concentration c and (ii) that the diffusion coefficient decreases when the liquid fraction increases. The first result is not so surprising since it has already been observed on single bubbles [7]. Moreover, most authors attribute the variation of the permeability with the concentration of surfactant to the higher difficulty for the gas to cross a denser interface. At concentrations higher than the cmc, the surface concentration does not depend on the bulk concentration anymore, explaining why no influence of the bulk concentration is observed.

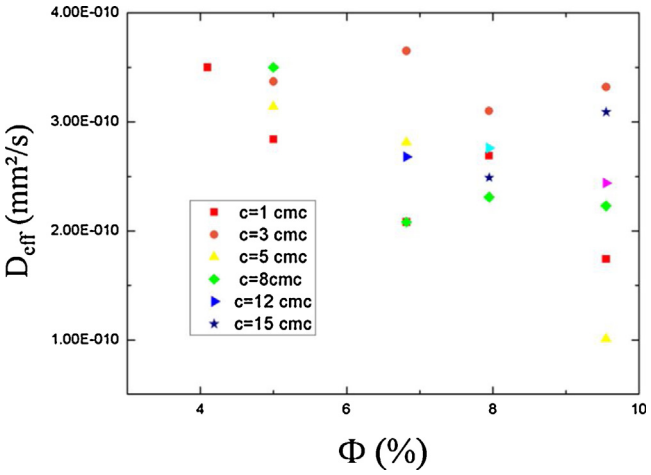

Fig. 6. Evolution of the diffusive coefficient with the liquid fraction for solutions of SDS of different concentrations.

The dependency of the diffusion coefficient on the liquid fraction is more pronounced and reflects different mechanisms. One of them is that the film height e_F decreases with the liquid fraction meaning that we cannot assume $e = e_F$ in Eq. (5). As it can be seen in Fig. 7, the actual height of the film (the flat part separating two bubbles) decreases when the radius of curvature r of the Plateau Borders increases. This thickness is the equivalent in 2D of the fraction of the area of the bubbles covered by the films in 3D [25]. This means that even if the permeability of the film does not depend on the liquid fraction, the coefficient D_{eff} should.

To take into account this effect, we used a semi-empirical approach to evaluate e_F:

- We measured, from a top view of the 2D foam, the variation of the radius R_{BP} of the pseudo-Plateau Border with the liquid fraction Φ.
- We deduced the value e_F from geometrical considerations [26]:

$$e_F = e - \sqrt{\frac{W_1 - (2\sqrt{3} - \pi)R_{\text{BP}}^2}{2 - (\pi/2)P_{\text{SQ}}}} \tag{8}$$

where W_1 is the quantity of liquid per bubble and P_{SQ} the mean perimeter of a bubble. This leads to the results presented in Fig. 7(b), which shows the film height as a function of the liquid fraction. One can see that e_F decreases linearly with the liquid fraction and does not depend on the surfactant concentration, as expected.

We used these values of e_F to normalise the effective diffusion coefficient and extract the permeability κ of the films. Taking into account the fact that $e \neq e_F$ the permeability becomes:

$$\kappa = \frac{e}{e_F}\frac{3P_0}{2\pi\gamma}D_{\text{eff}}. \tag{9}$$

We thus plotted the permeability, calculated from Eq. (9) and from the data of Fig. 6 as a function of the liquid fraction for different concentrations of SDS in Fig. 8. The new data does not exhibit a variation with the liquid fraction anymore. Nevertheless, the data are increasingly noisy when the liquid fraction increases. This is because the rearrangements occur more easily at high liquid fraction. The bubbles then reorganise before they disappear, hence changing topology (number of neighbours) and thus coarsening rate.

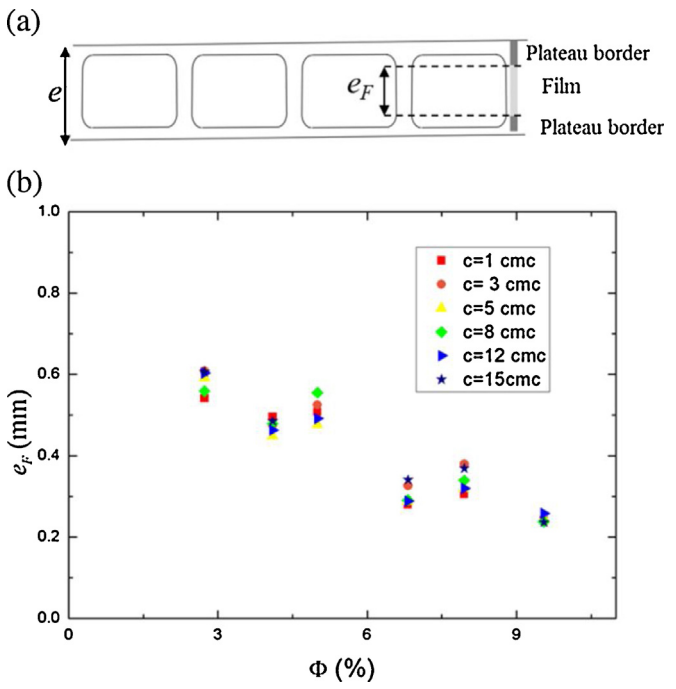

Fig. 7. (a) Side view of a 2D foam squeezed in between two plates separated by a thickness e. The height of the films depends on the liquid fraction and is denoted e_F. (b) Evolution of e_F with the liquid fraction Φ.

When the liquid volume fraction increases, the curvature of the Plateau borders decreases, hence the capillary pressure decreases. This capillary pressure $2\gamma/r$ is equilibrated by the disjoining pressure in the films, fixing the film thickness. In our experiments $\gamma \sim 35$ mN/m and $r \sim 0.4$–0.7 mm, the capillary pressure is thus around 100–175 Pa. Because the surfactant concentration is large, the Debye screening length is small and the disjoining pressure decreases very abruptly with film thickness. Around a disjoining pressure around 100–175 Pa, such as the one we estimated above, the film thickness is therefore expected to be largely independent of the liquid fraction and to remain between 10 and 20 nm as measured by Bergeron and Radke for SDS solutions at concentrations closed to the ones we use in this article [27]. As a consequence, we do not expect the film thickness to change appreciably in our experiments in the small range of capillary pressure explored.

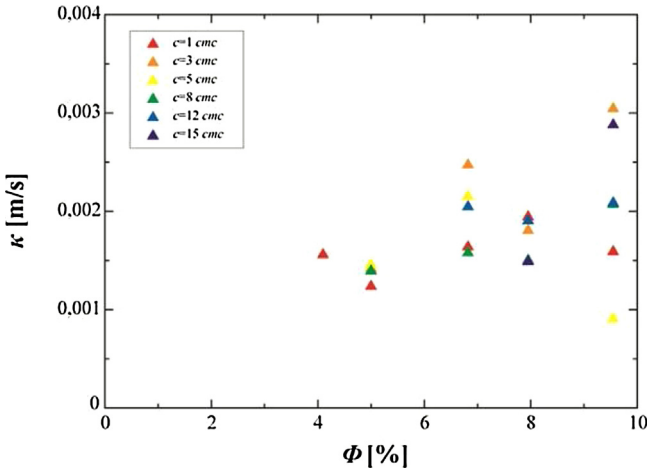

Fig. 8. Evolution of the permeability κ with the liquid fraction Φ for solutions of SDS of different concentrations c.

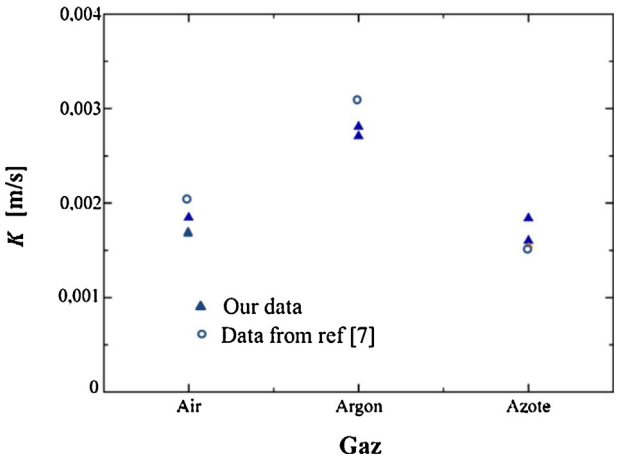

Fig. 9. In situ measurements of the permeability in SDS 2D foams (concentration of 3 cmc, liquid fraction of 6%) with different gas. Our data (filled triangles) are compared to data from the literature performed on single bubbles [7].

5.3. Influence of the gas

The method presented in the previous paragraph can now be applied to characterise the film permeability in various foams. Since neither the liquid fraction nor the surfactant concentration seems to impact the permeability, we choose to explore the influence of the gas.

The obtained permeabilities are shown in Fig. 9. We worked with air, argon and nitrogen with SDS at a surfactant concentration of three times the critical micellar concentration and a liquid fraction of 6%. We did the experiment twice for each gas to ensure reproducibility. The results are in line with previous measurements performed with the diminishing bubble method [7].

This shows that the collective behaviour of the bubbles is well taken into account in the von Neuman's law and validates the experiments at the scale of a single film or bubble. We thus provide a very simple method to measure the film permeability directly in a 2D foam since it is just necessary to count the number of bubbles along time and to know the initial average size of the bubbles A_0. Moreover, it is a reasonably fast method since only the very beginning of the coarsening process is analysed in the measurement.

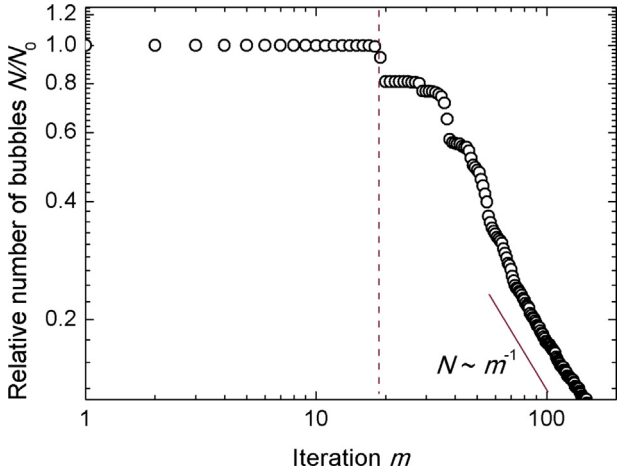

Fig. 10. Variation of number of bubbles with time all the way from an initially monodisperse foam to a polydisperse foam in the scaling state.

6. Conclusion

We have proposed a simple technique to measure the permeability of thin liquid films in quasi-2D foams by simply counting the number of bubbles squeezed between two plates and by following their evolution with time. By identifying the time interval after which most of the initially 5-sided bubbles disappear, one can determine in a straightforward manner the film permeability after taking properly into account the film height. We have shown that in the case of SDS this permeability is independent of the surfactant concentration above the cmc (in the range studied). It is also independent of the liquid fraction for the bubble sizes and liquid fractions investigated here.

In the future it would be interesting to use this experiment to systematically investigate the influence of the foam formulation on the film permeability. For instance, for surfactants exhibiting a disjoining pressure with a less abrupt barrier, the capillary pressure acting on the films may be sufficiently strong to influence the film thickness and therefore its permeability.

While for the coarsening investigations we have considered only the first catastrophic event, it may be interesting to consider in more detail what happens later. In fact, as shown in Fig. 10, the initially monodisperse foam undergoes several “dramatic events” before reaching the scaling state [2,15] in which the foam is completely disordered and polydisperse. In the latter state the number of bubbles is inversely proportional to time. It would be interesting to understand in more detail the physics of this transition following the work done by Duplat et al. [28]

Last but not least we would like to point out that the preliminary experiments conducted in order to ensure that we work with non-coalescing systems are not only important to choose regimes in which the foam bubbles do not coalesce but is also a first result in itself. The competition between coarsening and coalescence is an almost unexplored area and Fig. 3 shows that this competition depends not only on physical parameters (liquid fraction, bubble size, capillary pressure) but also on the surfactant concentration.

Acknowledgments

L.S. benefited from a CNES/CNRS PhD grant. We would like to thank Simon Cox for precious help with the Surface Evolver simulations. Part of this work was funded by the Centre National de Recherche Spatiale (CNES, GDR 2799), the European Space Agency (ESA, MAP project “Hydrodynamics of Wet Foams”) and the European Research Council (ERC) under the European Union’s Seventh Framework Program (FP7/2007–2013) in form of an ERC Starting Grant, agreement 307280-POMCAPS."

References

[1] I. Cantat, S. Cohen-Addad, F. Elias, F. Graner, R. Höhler, O. Pitois, Foams: Structure and Dynamics, Editions Belin, Paris Translation: Editions Oxford University Press, Oxford, 2013.
[2] D. Weaire, S. Hutzler, The Physics of Foams, Clarendon Press, Oxford, 1999.
[3] R. Farajzadeh, R. Krastev, P.L.J. Zitha, Foam film permeability: theory and experiment, Adv. Colloid Interface Sci. 137 (2008) 27–44.
[4] M. Nedyalkov, R. Krustev, D. Kashchiev, D. Platikanov, D. Exerowa, Permeability of Newtonian black foam films to gas, Colloid Polym. Sci. 266 (1988) 291–296.
[5] M. Nedyalkov, R. Krustev, A. Stankova, D. Platikanov, Mechanism of permeation of gas through Newton black films at different temperatures, Langmuir 8 (1992) 3142–3144.
[6] H. Princen, S. Mason, The permeability of soap films to gases, J. Colloid Sci. 20 (1965) 353–375.
[7] M. Ramanathan, H.J. Müller, H. Möhwald, R. Krastev, Foam films as thin liquid gas separation membranes, ACS Appl. Mater. Interfaces 3 (2011) 633–637.
[8] D. Exerova, P.M. Kruglyakov, Foam and Foam Films; Theory, Experiment, Application, Elsevier Science B.V., Amsterdam, 1998.
[9] R. Krustev, H.J. Muller, An apparatus for the measurement of the gas permeability of foam films, Rev. Sci. Instrum. 73 (2002) 398–403.
[10] R. Krustev, D. Platikanov, M. Nedyalkov, Permeability of common black foam films to gas. Part 2, Colloids Surf. A 123 (1997) 383–390.
[11] R. Krustev, D. Platikanov, M. Nedyalkov, Permeability of common black foam films to gas. Part 1, Colloids Surf. A 79 (1993) 129–136.
[12] V.T. Nguyen, D.D. Do, D. Nicholson, Solid deformation induced by the adsorption of methane and methanol under sub- and supercritical conditions, J. Colloid Interface Sci. 388 (2012) 209–218.
[13] A. Saint-Jalmes, M.-L. Peugeot, H. Ferraz, D. Langevin, Differences between protein and surfactant foams: microscopic properties, stability and coarsening, Colloids Surf. A 263 (2005) 219–225.
[14] S. Tcholakova, Z. Mitrinova, K. Golemanov, N.D. Denkov, M. Vethamuthu, K. Ananthapadmanabhan, Control of Ostwald ripening by using surfactants with high surface modulus, Langmuir 27 (2011) 14807–14819.
[15] I. Cantat, S. Cohen-Addad, F. Elias, F. Graner, R. Hohler, O. Pitois, F. Rouyer, A. Saint-Jalmes, Foams – Structure and Dynamics, Oxford University Press, Oxford, UK, 2013.
[16] A.E. Roth, C.D. Jones, D.J. Durian, Bubble statistics and coarsening dynamics for quasi-two-dimensional foams with increasing liquid content, Phys. Rev. E 87 (2013) 042304.
[17] G. Schliecker, Structure and dynamics of cellular systems, Adv. Phys. 51 (2002) 1319–1378.
[18] K. Brakke, The surface evolver, Exp. Math. 1 (1992) 141–165.
[19] A.-L. Biance, A. Delbos, O. Pitois, How topological rearrangements and liquid fraction control liquid foam stability, Phys. Rev. Lett. 106 (2011) 068301.
[20] V. Carrier, A. Colin, Coalescence in draining foams, Langmuir 19 (2003) 4535–4538.
[21] E. Rio, A.-L. Biance, Thermodynamic and mechanical timescales involved in foam film rupture and liquid foam coalescence, ChemPhysChem 15 (2014) 3692–3707.
[22] J.V. Neumann, Metal Interfaces, American Society for Metals, Cleveland, 1952.
[23] S. Cox, M. Fortes, Properties of three-dimensional bubbles of constant mean curvature, Philos. Mag. Lett. 83 (2003) 281–293.
[24] S. Cox, F. Graner, Three-dimensional bubble clusters: shape, packing, and growth rate, Phys. Rev. E 69 (2004) 031409.
[25] H. Princen, Osmotic pressure of foams and highly concentrated emulsions. I. Theoretical considerations, Langmuir 2 (1986) 519–524.
[26] C. Gay, P. Rognon, D. Reinelt, F. Molino, Rapid Plateau border size variations expected in three simple experiments on 2D liquid foams ⋆, Eur. Phys. J. E 34 (2011) 1–11.
[27] V. Bergeron, C.J. Radke, Equilibrium measurements of oscillatory disjoining pressures in aqueous foam films, Langmuir 8 (1992) 3020–3026.
[28] J. Duplat, B. Bossa, E. Villermaux, On two-dimensional foam ageing, J. Fluid Mech. 673 (2011) 147–179.